JCTC Journal of Chemical Theory and Computation

A QM/MM Exploration of the Potential Energy Surface of Pyruvate to Lactate Transformation Catalyzed by LDH. Improving the Accuracy of Semiempirical Descriptions

Silvia Ferrer,[#] J. Javier Ruiz-Pernía,[#] Iñaki Tuñón,*[,#] Vicente Moliner,*[,§] Mireia Garcia-Viloca,[‡] Angels González-Lafont,[‡,†] and José M. Lluch[‡,†]

Departament de Química Física/IcMol, Universitat de València, València, Spain, Departament de Ciències Experimentals, Universitat Jaume I, Castelló, Spain, Institut de Biotecnologia i de Biomedicina, Universitat Autònoma de Barcelona, Spain, and Departament de Química, Universitat Autònoma de Barcelona, Barcelona, Spain

Received February 2, 2005

Abstract: We present a QM/MM study of the potential energy surface of the pyruvate to lactate transformation catalyzed by L-lactate dehydrogenase. The transformation involves a hydride and a proton transfer which are followed by means of the corresponding antisymmetric combination of the distances from the hydrogen atom to the donor and the acceptor atoms. To discriminate among the possible reaction mechanisms we have considered different improvements of the AM1/MM description: reoptimization of the van der Waals parameters and inclusion of corrections to the QM energy associated with both transfer coordinates. The QM subsystem has been also enlarged to include charge-transfer effects from the substrate to some specific residues. In our best treatment, the transformation is described as a concerted process through a single transition structure in which the hydride transfer is more advanced than the proton transfer. From the methodological point of view, the correction schemes tested here improve the quality of the semiempirical potential energy surface although they also present deficiencies attributed to consideration of the proton and hydride transfer corrections as separable ones.

1. Introduction

L-Lactate dehydrogenase (LDH) is a highly stereospecific metabolic enzyme which catalyzes the interconversion of pyruvate and L-lactate using the NADH/NAD^+ pair as redox cofactor. Formally, the reaction in the pyruvate → L-lactate direction is achieved by reducing the carbonyl group with a hydride anion transferred from NADH and a proton transfer from a protonated His195 residue:[1]

$$CH_3COCOO^- + NADH + H^+ \rightleftharpoons CH_3CH(OH)COO^- + NAD^+$$

Much information on the mechanism has come from kinetic and site-directed mutagenesis experiments.[2] These studies characterize the enzyme (structure and details about the active site and mechanism) setting up that, while in the wild-type enzyme the rate-limiting step of both, the pyruvate reduction or the lactate oxidation process is a unimolecular rearrangement of the enzyme−NADH−pyruvate complex, and the rate of catalysis in the mutants is limited by the chemical reaction. In this regard, it is still unknown whether the reaction mechanism involves sequential proton and hydride ion transfers or if both transfers take place in a concerted way (see Scheme 1). The difference in the timing of the hydride transfer and the proton transfer is a matter of interest in mechanistic enzymology. Computational studies from different groups[3−7] suggested that the sequential mechanism is more likely, but the proposals differ in the order in which the proton and hydride ions are transferred. Thus, Ranganathan and Gready[6,7] found a mechanism in which the hydride transfer preceded proton transfer in a stepwise

* Corresponding authors e-mail: tunon@uv.es (I.T.) and moliner@exp.uji.es (V.M.).
† Departament de Química, Universitat Autònoma de Barcelona.
‡ Institut de Biotecnologia i de Biomedicina.
§ Universitat Jaume I.
# Universitat de Valencia.

10.1021/ct050016l CCC: $30.25
Published on Web 05/10/2005

Scheme 1

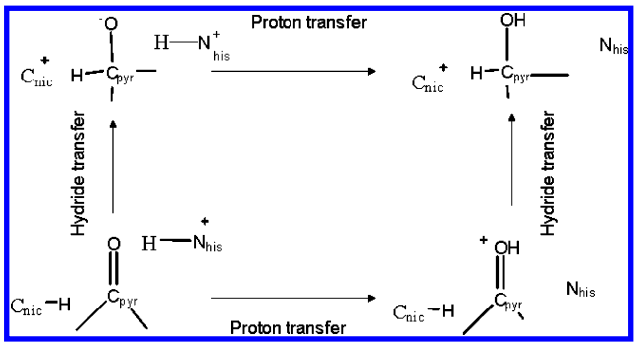

manner, in accordance with a previous study by Warshel et al. using an empirical valence bond study,[8] but contrasting with the usual chemical and enzymatic arguments for hydride transfer processes and with other theoretical studies[3,4,8] that predicted a concerted but asynchronous reaction in which the proton transfer was in a very advanced stage of the reaction. Finally, a more flexible quantum mechanical/molecular mechanical (QM/MM) treatment[5] allowed tracing the two distinct reaction pathways across the energy hypersurface. Nevertheless, as it was pointed out in this study,[5] the results at this point did not allow for making a definitive statement as to which mechanism was preferred. Without considering the fact that accurate determination of transition state properties would require statistical averaging over many configurations, each one individually being a transition state structure,[5,9] the previous study presented a limitation since a semiempirical Hamiltonian was employed to describe the quantum region. This, together with the fact that both pathways presented similar energy barriers, prevented to answer the question of which mechanism was preferred. To get more reliable energetics thus allowing to answer this question, a higher level of theory should be used in the QM/MM calculations.

Because of the reasons mentioned above, this enzymatic reaction provides an excellent example to illustrate the need of improving the accuracy of the QM/MM methods where the QM region is described by means of semiempirical Hamiltonians. One of the final goals of a theoretical study is usually to obtain the free energy profile of the desired enzymatic reaction. This free energy profile can be compared to experimental data and is also a powerful tool to get a deeper insight into the different contributions to catalysis. Obviously, the quality of these calculations is determined by the accuracy of the potential energy surface employed to describe the process. In the current example the selection of a theoretical level can be decisive to favor one or another reaction path. The conclusions reached by a theoretical study will be relevant only if we can be confident on the quality of our theoretical method to describe with similar accuracy different possible reaction mechanisms. This purpose is obviously limited by the computational cost. High level quantum potential energy and gradient calculations for medium-sized systems interacting with a large classical environment are still prohibitive taking into account that optimizations in highly dimensional energy surfaces require hundreds or even thousands of steps. In this paper we test different correction schemes in order to improve semiempirical descriptions at a low additional computational cost. These schemes are applied to discern between the two possible reaction mechanisms appearing on the semiempirical potential energy surface. We also address the other questions affecting the accuracy of the QM/MM calculations such as the optimization of the van der Waals parameters for the interaction between the QM and the MM subsystems and the size of the QM region. Considering all these aspects, and bearing in mind the limitations of the computational approach, the most favored reaction mechanism for the pyruvate to lactate transformation catalyzed by LDH in our treatment is a concerted but asynchronous mechanism where the hydride transfer is more advanced that the proton transfer at the transition state structure. Mechanistic details are dependent on the computational level chosen to describe the reaction.

2. Theory

In the present work, we have modeled the potential energy surface (PES) by a combined quantum-mechanical and molecular-mechanical (QM/MM) approach[10,11] that includes the generalized hybrid orbital (GHO)[12] method to treat the boundary between the quantum-mechanical (QM) and the molecular-mechanical (MM) fragments of the system. We used the semiempirical Austin model 1 (AM1)[13] to describe the QM subsystem. A semiempirical description can be quite inaccurate in some cases, and its use requires the previous calibration of the Hamiltonian. Obviously, it would be ideal to use a higher level ab initio molecular orbital or density functional theory (DFT) method to represent the reactive part of the system. However, these calculations are still too time-consuming to be practical at the present time for enzymatic systems considering that PES exploration, location, and characterization of stationary structures and molecular dynamics simulations (if needed) may require thousands of energy and gradient evaluations. An alternative dramatic reduction of the MM region size would not be realistic as the effect of long-range interactions as well as the flexibility of the system would be lost. There are several alternatives to improve the semiempirical description at a moderate or negligible computational cost. In principle one can develop specific reaction parameters (SRP)[14] designed to reproduce higher level results or to include correction energy terms to the original PES. We have here employed two of this last kind of methods.

As explained before we are interested in a chemical process which is composed of two elementary chemical steps: a hydride transfer and a proton transfer. These hydrogen transfers are here described using as reaction coordinates the antisymmetric combination of the distances from the hydrogen atom to the donor (r_{DH}) and the acceptor (r_{AH}) atoms:

$$R = r_{DH} - r_{AH}$$

We will use the symbols R_1 for the hydride transfer and R_2 for the proton transfer (see below for details). We will consider in this work two independent corrections to the semiempirical electronic energy associated with each one of these two coordinates.

The two correction methods used in this work are carried out by introducing two energy terms, which are functions that depend exclusively on R_1 and R_2 reaction coordinates, respectively.

The first correction method is the Simple Valence Bond (SVB)[15,16] In this method, the total potential energy of the system is given by the following equation

$$E_{tot} = E_{qm} + E_{mm} + E_{qm/mm} + E_{SVB,R1} + E_{SVB,R2} \quad (1)$$

where E_{qm} is the energy of the QM subsystem, E_{mm} is the energy of the MM subsystem, $E_{qm/mm}$ is the interaction energy between the QM and the MM regions, which include both electrostatic and van der Waals terms, and the E_{SVB} terms represent the SVB correction to the semiempirical E_{qm} energy in a particular reaction coordinate R_i. The following function has been proposed for this correction term

$$E_{SVB,Ri}(r_{DH}, r_{DA}, r_{AH}) = \frac{1}{2}[M_1(r_{DH}) + M_2(r_{AH})] - \frac{1}{2}([M_1(r_{DH}) - M_2(r_{AH})]^2 + 4[V_{12}(r_{DA})]^2)^{1/2} + \Delta D_{DH} \quad (2)$$

where r_{DA} is the distance between the donor and the acceptor atoms, the function V_{12} is given by

$$V_{12}(r_{DA}) = D_{DA}\exp[-\alpha_{12}(r_{DA} - r^0_{DA})] \quad (3)$$

and

$$M_i(r_{XH}) = \Delta D_{XH}(\exp[-2\alpha_{XH}(r_{XH} - r^0_{XH})] - 2\exp[-\alpha_{XH}(r_{XH} - r^0_{XH})]) \quad (4)$$

where XH represents the different pairs of atoms: donor-hydrogen (DH) or acceptor-hydrogen (AH) in the Morse potentials M_1 and M_2, respectively, and r^0_{XH} is the equilibrium distance of the corresponding bond. We set the two values ΔD_{XH} equal to the difference in dissociation energy between a high level theory calculation (in this work we use second-order Moller Plesset (MP2) level of calculation with a 6-31+G(d) basis set) and the lower level (the AM1 semiempirical method); α_{XH} is calculated as

$$\alpha_{XH} = \left(\frac{k_{XH}}{2D^0_{XH}}\right)^{1/2} = \upsilon_{XH}\left(\frac{2\pi^2\mu}{D^0_{XH}}\right)^{1/2} \quad (5)$$

where D^0_{XH} is the bond energy, μ is the reduced mass of atoms X and H, and k is the force constant. The parameters D_{DA} and α_{12} in eq 3 are adjusted to obtain the desired barrier height, which is the barrier height calculated at the higher level in gas phase.

The second correction method is the interpolated corrections (IC) scheme based on the use of cubic splines under tension.[17] The total potential energy is given by the following equation:

$$E_{tot} = E_{qm} + E_{mm} + E_{qm/mm} + \Delta E_{IC}(R_1) + \Delta E_{IC}(R_2) \quad (6)$$

This correction term is obtained as the difference between the qm energy provided by the high level method (HL) and the low level (LL) one for a particular configuration of the system obtained along the chosen reaction coordinate (R_i).

$$\Delta E(R_i) = E^{HL}_{QM}(R_i) - E^{LL}_{QM}(R_i) \quad (7)$$

Several structures are selected to calculate the energy difference between the high level and the low level methods at different values of the R_i coordinates. Then, following the work of Truhlar et al.,[18,19] a spline under tension is used to interpolate this correction term at any value of R_i. In this way we obtain a continuous function in R_i, with continuous first and second derivatives, which are necessary to perform molecular dynamics simulations. To preserve the general applicability of the method the spline fit is carried out in terms of a mapping coordinate z, defined as

$$z_i = \frac{2}{\pi}\arctan\left(\frac{R_i - R_{i0}}{L}\right) \quad (8)$$

The new variable allows us to map the energy correction term onto the finite interval $[-1,+1]$. The constants R_{i0} and L are chosen for centering and scaling the mapping function in the range of interest.[19] Then the final interpolated correction is obtained as

$$\Delta E_{IC}(R_i) = \text{spline}\{\Delta E[z_i(R_i)]\} \quad (9)$$

3. Calculations and Computational Details

3.1. Model of the Enzyme−Substrate−Coenzyme Complex. The X-ray structure of lactate dehydrogenase from *Bacillus stearothermophilus* comes from the PDB code 1LDN which is an octamer, although in this work only the tetramer is used (Figure 1). X-ray studies have proposed that the tetramer is the functional form of lactate dehydrogenase from *Bacillus stearothermophilus.*[20] In each monomer the crystal structure contains a total of 316 amino acid residues, the cofactor NADH, and the inhibitor oxamate (OXM), which is replaced by pyruvate in our study.

The coordinates of the hydrogen atoms of the protein and coenzyme were determined using the HBUILD facility of the CHARMM package.[21] All the ionizable groups were set to their normal ionization state at pH 7 with the exception of His195, which was modeled in its protonated form. Other histidine residues of the protein were modeled as neutral with the proton at Nδ.

Then, the system was partitioned into a quantum mechanical region consisting of 52 atoms and a molecular mechanical region containing the rest of the system. The QM subsystem includes 9 atoms of the pyruvate, 13 atoms of the His195 residue (including the C_α as a boundary atom), and 30 atoms of the NADH, which include the dihydronicotinamide and ribose rings, and the C5′ ribose atom as a boundary atom. The QM subsystem is described using the AM1 Hamiltonian and the boundary atoms are represented by the GHO method. A picture of the active site showing the partition into QM and MM subsystems is presented in Figure 2. First, the total energy of the system was minimized for 20 steps with the Adopted Basis Newton−Raphson (ABNR)[21] method by moving only the QM part of the system. Then, the system was solvated with a 24 Å radius sphere of TIP3P[22] water molecules centered on the pyruvate center of mass (see Figure 1). Water molecules that were within 2.5 Å of any non-hydrogen atom were removed. The

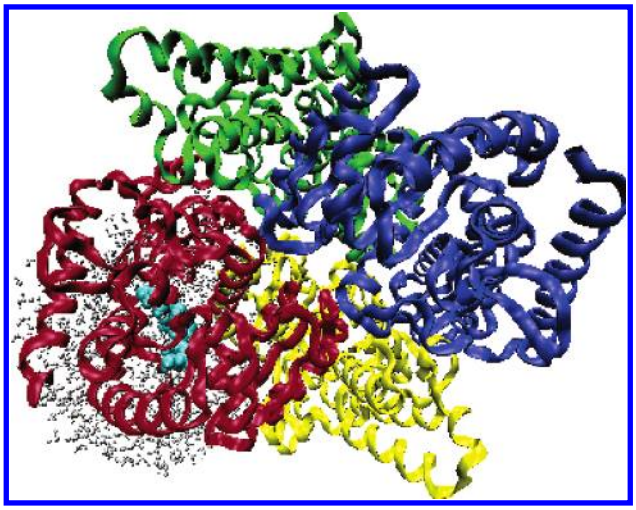

Figure 1. Tetramer of LDH with one of the active sites (NADH, pyruvate, and His-195) in blue balls. A sphere of water molecules with a radius of 24 Å water molecules has been centered on the center of mass of pyruvate.

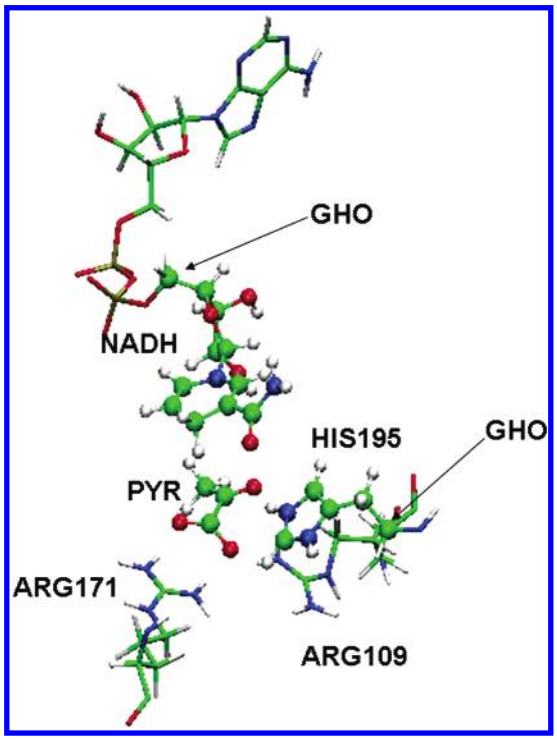

Figure 2. Snapshot of the LDH active center with the substrate (pyruvate) and the cofactor (NADH): The QM region is represented using balls and sticks. The position of the GHO atoms used to define the boundary with the MM region is also indicated.

resulting system was resolvated four more times using different relative orientations between the protein and the water sphere to ensure a good solvation of the system. Then, water positions were optimized for 20 steps followed by the optimization of the geometry of the part of the system included in a sphere of 24 Å. Finally, a molecular dynamics simulation of the waters (5 ps) was carried out to relax energetically unfavorable contacts, and the 3-fold cycle of superposition, deletion, and rotation was then repeated to fill in additional cavities generated during the dynamics simulation. The final model has 22 139 atoms, 19 862 of them are atoms from the protein or the ligands, and the rest, 2277, are atoms from the water molecules.

3.2. Reaction Coordinates. As explained before two reaction paths have been proposed in previous studies[5] (see Scheme 1). The first one is a mechanism where the hydride transfer precedes the proton transfer. This mechanism has been described as stepwise, where the initial step is the hydride transfer from a carbon atom of dihydronicotinamide, C_{nic} (donor atom), to the carbonyl carbon atom of pyruvate, C_{pyr} (acceptor atom), and in a second step a proton is transferred, from the N atom of His195, N_{his} (donor atom), to the carbonyl oxygen atom of pyruvate, O_{pyr} (the acceptor atom). The second proposed mechanism is a concerted but asynchronous mechanism where the proton and the hydride transfer take place through a single transition state (TS), being as how the proton transfer is now more advanced than the hydride transfer. For clarity purposes we will denote these two mechanisms as the hydride plus proton transfers pathway (the HP Pathway) and the proton plus hydride transfer pathway (the PH Pathway), respectively. Both mechanisms can be described on a single PES obtained as a function of two reaction coordinates (see Scheme 1). The reaction coordinate R_1 for the hydride transfer is defined in this work as the difference in the distances of the bonds between the transferring hydride-ion and the donor (C_{nic}) and the acceptor (C_{pyr}) atoms (eq 10). For the proton transfer a reaction coordinate R_2 is defined as the difference in the distance of the bonds between the transferring proton and the donor (N_{his}) and the acceptor (O_{pyr}) atoms (eq 11)

$$R_1 = r_{C_{nic}H_1} - r_{C_{pyr}H_1} \tag{10}$$

$$R_2 = r_{N_{his}H_2} - r_{O_{pyr}H_2} \tag{11}$$

The exploration of the PES was then carried out using the R_1 and R_2 coordinates defined before. These coordinates seem a reasonable choice to define a reduced PES, as they change smoothly along the surface. However, it must be taken into account that reduced surfaces give approximate descriptions of chemical processes. The CHARMM program was employed to carry out this exploration by means of the use of the RESDISTANCE keyword to define the reaction coordinates (R_i).

3.3. Exploration of the Potential Energy Surfaces. In this work, we have calculated two-dimensional (2D) potential energy surfaces (PES) at four different levels of theory: the uncorrected AM1/MM, the AM1-SVB/MM, the AM1-IC/MM, and the 2D-MP2sp/MM (bidimensional single-point calculations at the MP2 level). Gradient and energy calculations have been performed for the first three methods, whereas the 2D-MP2sp/MM is the result of single-point energy calculations on the AM1/MM optimized structures.

During all the optimizations, those atoms 24 Å away from the active site, 14 996 atoms, were kept frozen in order to reduce the computational cost, while 7143 atoms were allowed to move. In all the cases, the total energy of the system was minimized with the ABNR[21] method until the norm of the gradient with R_1 and R_2 directions projected out was less than 0.001 kcal mol^{-1}·$Å^{-1}$.

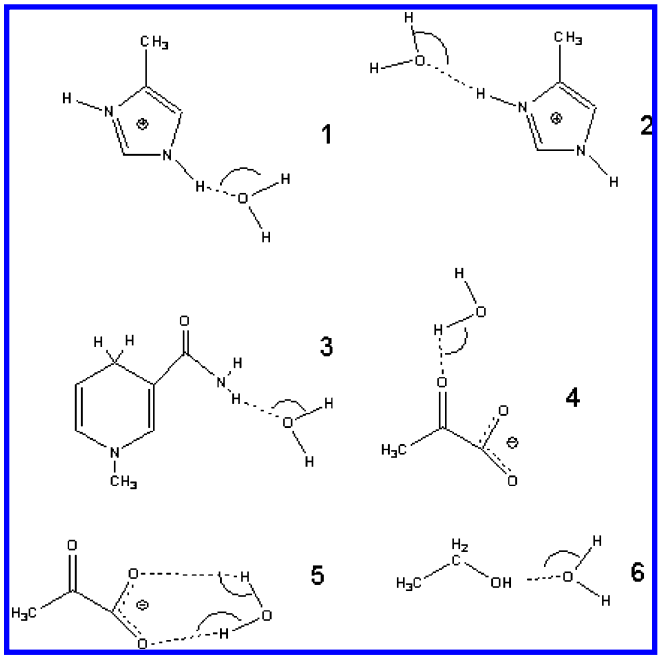

Figure 3. Bimolecular complexes of histidine fragment, nicotinamine ring model, pyruvate, and ethanol with water molecules.

3.4. QM/MM van der Waals Parameters. Prior to the PES exploration we have recalibrated the QM/MM potential by adjusting the van der Waals parameters of the QM atoms, employed to evaluate the interaction with the MM region. With this purpose we have obtained the interaction energy between some molecules that mimic the QM molecules and TIP3P water molecules by the procedure described by Freindorf and Gao.[23] We have considered complexes of water with models of the histidine and nicotinamide rings, with pyruvate and with ethanol to optimize the van der Waals parameters of the nitrogen atoms, hydroxyl oxygens, polar hydrogens bonded to nitrogen or oxygen, and also the carbon and oxygen atoms of pyruvate. Figure 3 shows the bimolecular complexes used to calculate the intermolecular interaction energy. The calculations were carried out describing all the complexes using quantum mechanics, at the HF/6-31G(d) level of theory and also using a hybrid QM/MM scheme where water molecules were described using TIP3P and the rest of the complex at the AM1 level. In all cases we have frozen the internal degrees of freedom of the QM fragments at gas-phase optimized values at the corresponding QM level, while the water intramolecular parameters have been fixed to the experimental geometry. To reproduce the HF/6-31G(d) results we have only modified the Lennard-Jones parameters, ϵ_{ab} and σ_{ab}, of selected QM atoms in the QM/MM interaction Hamiltonian $H_{qm/mm}$. As starting values for the Lennard-Jones parameters we used those provided by Gao and co-workers.[24] Table 1 provides the total interaction energies of the complexes at the HF level and also using QM/MM calculations with the van der Waals parameters obtained from the CHARMM force field, from Gao and co-workers, or after our optimization procedure. As it can be seen, in Table 1 we improved the energetic description of the complexes established with the histidine fragment and ethanol changing the parameters associated with nitrogen, oxygen, H(N), and H(O) atoms. However, we were not able to reproduce the full QM interaction with the carbon and oxygen atoms of pyruvate following this scheme. The reason for this behavior could be related to the noninclusion of charge transfer effects in our QM/MM Hamiltonian between pyruvate and water molecules. The magnitude of the charge transfer term is probably too big to be accounted by fitting the van der Waals parameters. The importance of the charge-transfer effect in pyruvate will be further addressed below. The original CHARMM parameters, those of ref 24, and the optimized ones are listed in Table 2. Geometries and absolute energies at the HF/6-31G(d) level of the complexes are given as Supporting Information.

Table 1. Total Interaction Energies (in kcal/mol) for the Complexes Appearing in Figure 3[a]

complex no.	ΔE(HF)	ΔE(1)	ΔE(2)	ΔE(3)
1	−16.02	−12.92	−13.9	−15.82
2	−16.18	−13.03	−14.03	−15.98
3	−5.24	−5.03	−5.07	−5.62
4	−10.81	−14.74	−14.84	−14.84
5	−13.02	−17.63	−17.68	−17.68
6	−5.47	−3.17	−3.80	−3. 89

[a] Each column shows the results obtained at the HF/6-31G(d) level of theory and at the AM1/MM level using the van der Waals parameters of the CHARMM force field (1), those provided in ref 24 (2), and the optimized parameters (3) given in Table 2.

3.5. Evaluation of Corrections to the Potential Energy. To improve the performance of the AM1 model through the use of the SVB or IC schemes, we carried out gas-phase ab initio calculations for smaller model reactions (Figure 4): In the selected model, 42 atoms constitute the three species that are involved in the two chemical processes: the hydride and the proton transfer. In a previous study[3−5] of the same reaction, where we used a smaller model for the enzyme−substrate system (LDH monomer), the stationary points were localized on a AM1/MM potential energy surface. Here, we have used the stationary points of the HP Pathway to cut the Cartesian coordinates for the 42 atoms of the gas-phase model (Figure 4). The Cartesian coordinates for additional

Table 2. van der Waals Parameters for the Quantum Atoms[e]

	this work		Gao et al.[a]		CHARMM	
atom	σ	ϵ	σ	ϵ	σ	ϵ
N(H)/N(H2)[b]	1.00	−0.14	1.57	−0.15	1.85	−0.20
H(N)[b]	0.35	−0.08	0.45	−0.10	0.2245	−0.046
H(O)[b]	0.28	−0.10	0.45	−0.10	0.2245	−0.046
O(H)[b]	1.08	−0.08	1.65	−0.20	1.70	−0.12
C(═O)[b]	1.65	−0.20	1.65	−0.20	1.70	−0.12
C(H)[b]	1.96	−0.08	1.96	−0.08	1.99	−0.07
O(═C)[b]	1.65	−0.20	1.65	−0.20	1.70	−0.12
O[c]	1.65	−0.20	1.65	−0.20	1.70	−0.12
H[d]	1.12	−0.01	1.12	−0.01	1.32	−0.022

[a] Reference 24. [b] A(B) stands for atoms A bound to atom or group B. [c] Oxygen of a carboxylate group. [d] On C. [e] The parameters are given according to the criteria of the CHARMM force field in Å and kcal/mol.

structures between have been obtained from AM1/MM optimizations at different values of the R_1 and R_2 coordinates on the LDH monomer model. Then, we have carried out single-point calculations on the 42 atoms gas-phase model at the AM1 level and by including electron correlation at the second-order Moller−Plesset perturbation theory with a polarized split valence basis set (MP2/6-31G(d,p)). The GAUSSIAN98[25] and CHARMM[21] programs were used for these calculations. Table 3 gives the gas-phase relative energies calculated at the AM1 and MP2 levels. From comparison between semiempirical and MP2 values a non-negligible error can be expected when obtaining the PES of the enzymatic process using the AM1 Hamiltonian. In particular, the use of these Hamiltonian results in a single-point recalculated reaction energy about 26 kcal/mol higher for the hydride transfer and a single-point recalculated reaction energy about 18 kcal/mol lower for the proton transfer. It also produces an important error in the hydride transfer barrier (the difference in the single-point recalculated barriers is 16.9 kcal/mol). Thus, consideration of correction schemes seems to be necessary to improve the accuracy of our computational model. The parameters determined for the SVB correction terms (see eqs 1−5) using these values are shown in Table 4.

For the IC method, we used the same gas-phase results on the 42 atoms model (Figure 4) to determine the two correction terms as a function of R_1 and R_2, respectively. For a given value of R_1 or R_2 the correction term is the difference between the single-point potential energy obtained using high level (MP2) and low level (AM1) methods. Two independent cubic splines are used to fit the correction energies as a function of the reaction coordinates (R_i).

It must be pointed out that according to the procedure described the structures selected to parametrize both correction schemes are obtained from the same region of the PES (if we divide the PES presented in Scheme 1 with a diagonal traced from reactants to products, the selected structures have been taken exclusively from the upper half part), and thus the correction procedures are expected to work more properly in this region. This important limitation will be discussed in more detail later on.

4. Results

4.1. Potential Energy Surfaces. Figure 5 shows the PES obtained using R_1 and R_2 coordinates at the AM1/MM level without corrections. The PES shows two distinct mechanistic pathways with very similar features to those found in a previous work on the LDH monomer using link atoms instead of GHO.[5] The hydride plus proton transfer pathway (HP Pathway) is a stepwise mechanism involving first the hydride transfer from the dihydronicotinamide ring of the NADH to a carbon atom of pyruvate followed by a proton transfer from the protonated His195 to the carbonyl O atom of pyruvate. On the other hand, the proton plus hydride transfer pathway (PH Pathway) is a concerted mechanism in which the proton transfer is considerably more advanced than the hydride transfer in the transition state (TS3). Table 5 gives the most relevant bond distances and the relative energies of the stationary points located on the AM1/MM PES. From the values of the distances given in Table 5 it is evident that TS1 corresponds to the hydride transfer where the proton transfer has been only slightly advanced. TS2 is the transition state structure associated with the proton transfer once the hydride has been already transferred. TS3 is the transition state structure associated with a concerted but very asynchronous proton and hydride transfers, where the proton transfer is considerably more advanced than the hydride transfer. The energy barriers for the HP Pathway are about 52 kcal/mol from reactants (pyruvate) to the intermediate and 14 kcal/mol from the intermediate to products (lactate), while the energy barrier in the PH Pathway is about 41 kcal/mol. Thus, on the AM1/MM PES the PH Pathway is the favored mechanism but taking into account the expected errors of the AM1 description, these results are still inconclusive about the preferred mechanism for the pyruvate to lactate transformation.

Figure 6 shows the PES calculated with the inclusion of the two SVB correction terms. As it can be seen it is possible to define again the two same mechanisms with similar features. Thus, the HP Pathway is a stepwise mechanism presenting an intermediate after the hydride transfer, and the PH Pathway is a concerted but asynchronous process. The differences with respect to the uncorrected AM1/MM PES appear in the relative energies of the stationary structures. In the HP Pathway the energy barriers are of about 29 kcal/mol from reactants (pyruvate) to intermediate (TS1) and about 11 kcal/mol from intermediate to products (TS2)—see Table 6. In the PH Pathway the energy barrier is again about 41 kcal/mol. We can stress at least two important conclusions at this point. First, the energy barriers now found seem to be more reasonable for an enzymatic process as they are considerably lower than in the uncorrected exploration. Second, while the PH Pathway presents a lower energy barrier on the uncorrected AM1/MM PES, now the prevalence of the HP Pathway is quite clear, because it presents noticeably lower energy barriers. The preference for this mechanism was clearly established by means of PES explorations carried out using a symmetric combination of the R_1 and R_2 coordinates. Starting from both, the reactants or the products, and using this new distinguished reaction coordinate, the chemical transformation always took place

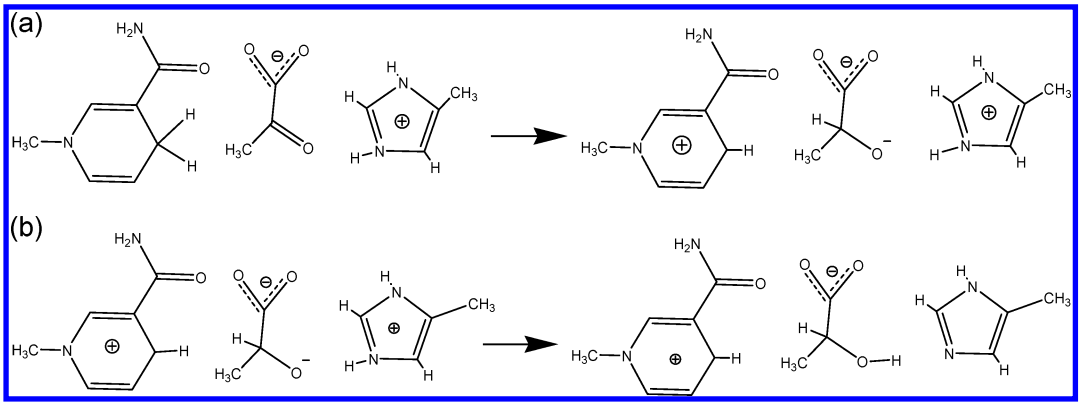

Figure 4. Molecular models used to calibrate the performance of the AM1 method versus MP2/6-31G(d,p) calculations: (a) model used for the hydride transfer reaction: from reactants (NADH and pyruvate) to intermediate (NAD^+ and $PyrH^-$) and (b) model used for the proton-transfer reaction: intermediate ($PyrH^-$ plus protonated His195) to products (lactate and His195).

Table 3. Single-Point (SP) Recalculated Gas-Phase Reaction Energies and Barrier Heights (kcal/mol) for the Hydride-Transfer Reaction and the Proton-Transfer Reaction in the Molecular Model Presented in Figure 4[a]

	SP recalculated barrier	SP recalculated reaction energy
	Hydride Transfer	
AM1	76.27	93.11
MP2/6-31G(d,p)	59.38	66.96
	Proton Transfer	
AM1	−5.07	−61.57
MP2/6-31G(d,p)	−7.07	−43.14

[a] Recall that the geometries are taken from AM1/MM calculations.

Table 4. Parameters of the SVB Functions for the Hydride (a) and Proton Transfer Steps (b)[a]

(a)

ΔD_{DH}	α_{DH}	ΔD_{AH}	α_{AH}	D_{DA}	α_{DA}
0.01	1.36	26.15	6.43	1.5	0.50

(b)

ΔD_{NH}	α_{NH}	ΔD_{OH}	α_{OH}	D_{NO}	α_{NO}
21.27	1.49	1.46	1.09	7.1	1.00

[a] ΔDs are given in kcal/mol and α in $Å^{-1}$.

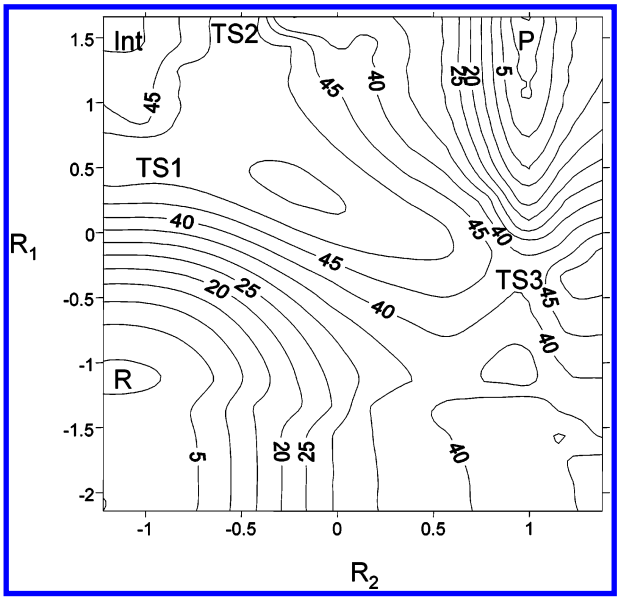

Figure 5. Potential energy surface at the AM1/MM level. R_1 and R_2 are the coordinates (in Å) associated with the hydride and proton transfers (see eqs 10 and 11). The position of reactants (R), intermediate (Int), products (P), and transition state structures (TS1, TS2, and TS3) is qualitatively shown. Isoenergetical lines are depicted each 5 kcal/mol.

through the HP Pathway. The energy profiles obtained using the R_1+R_2 coordinate are provided as Supporting Information.

Figure 7 shows the PES calculated with the inclusion of ICs through the use of two independent cubic splines associated with the R_1 and R_2 coordinates. The obtained PES is very similar to the previous one. In fact, by inspection of the PES it is possible to define again the two same reaction mechanisms. Thus, the HP Pathway is a stepwise mechanism and the PH Pathway is a concerted one. The energy barrier for the hydride transfer in the HP Pathway is of about 34 kcal/mol —see Table 7—while for the subsequent proton transfer is of about 11 kcal/mol (from the intermediate). In the PH Pathway the energy barrier is about 52 kcal/mol. Therefore, also within this correction methodology the preferred mechanism is the HP Pathway. Differences with respect to the previous methodology are found in the geometry of the stationary structures. Thus, reactants are now found at larger distances from pyruvate atoms to the hydride and the proton. However, these changes are not very relevant in energy as the reactants are found in a very flat valley, and then its exact position can change noticeably depending on the particularities of the energy function employed. Geometrical changes are also found in the structure of TS3 with respect to the SVB surface. On this new PES the TS3

Table 5. Relevant Distances (Å) and Relative Energies (kcal/mol) of the Stationary Structures Appearing on the AM1/MM PES

	$r_{C_{nic}H_1}$	$r_{C_{pyr}H_1}$	$r_{N_{his}H_2}$	$r_{O_{pyr}H_2}$	energy
reactants	1.15	2.29	1.00	2.22	0
TS1	1.70	1.24	1.01	2.03	52
intermediate	2.80	1.15	1.00	2.22	38
TS2	2.79	1.14	1.06	1.68	52
products	2.79	1.13	1.98	0.99	−5
TS3	1.30	1.44	1.96	0.99	41

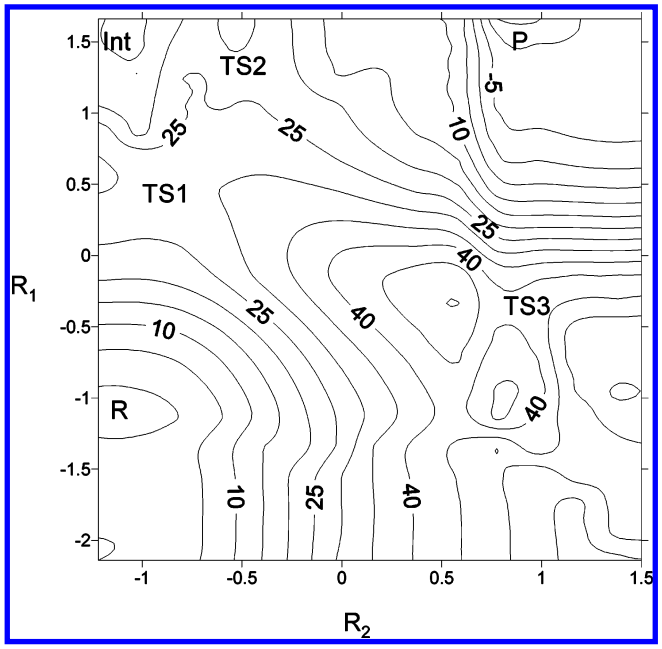

Figure 6. Potential energy surface at the AM1-SVB/MM level. R_1 and R_2 are the coordinates (in Å) associated with the hydride and proton transfers, respectively (see eqs 10 and 11). The position of reactants (R), intermediate (Int), products (P), and transition state structures (TS1, TS2, and TS3) is qualitatively shown. Isoenergetical lines are depicted each 5 kcal/mol.

Table 6. Relevant Distances (Å) and Relative Energies (kcal/mol) of the Stationary Structures Appearing on the PES Obtained at the AM1/MM Level with the Inclusion of SVB Correction Terms

	$r_{C_{nic}H_1}$	$r_{C_{pyr}H_1}$	$r_{N_{his}H_2}$	$r_{O_{pyr}H_2}$	energy
reactants	1.14	2.29	1.01	2.03	0
TS1	1.62	1.16	1.00	2.02	29
intermediate	2.79	1.13	1.01	2.03	14
TS2	2.79	1.13	1.06	1.67	25
products	2.79	1.13	1.96	0.98	−15
TS3	1.21	1.55	1.77	0.99	41

structure appears at slightly less advanced values of the hydride and proton-transfer coordinates.

At this point it is important to stress the fact that the two correction schemes display very similar behavior because they have been parametrized to reproduce the same high level quantum method energies using structures taken from the same region of the uncorrected PES. As described above, the reference structures used to obtain the correction energies were selected from the HP Pathway of an uncorrected PES. Thus, it would be reasonable to question the ability of the two methods to give accurate predictions of the PES in the region corresponding to the PH Pathway. For this reason we decided to obtain a new corrected PES based on bidimensional energy single-point calculations at the MP2/6-31G(d,p) level using the gas-phase model in Figure 4 and taking the geometries from the AM1/MM-2D PES (Figure 5). This new PES was obtained using the following energy function

$$E = E_{AM1} + E_{AM1/MM} + E_{MM} + (E'_{MP2} - E'_{AM1}) \quad (12)$$

where E' are the result of single-point energy calculations

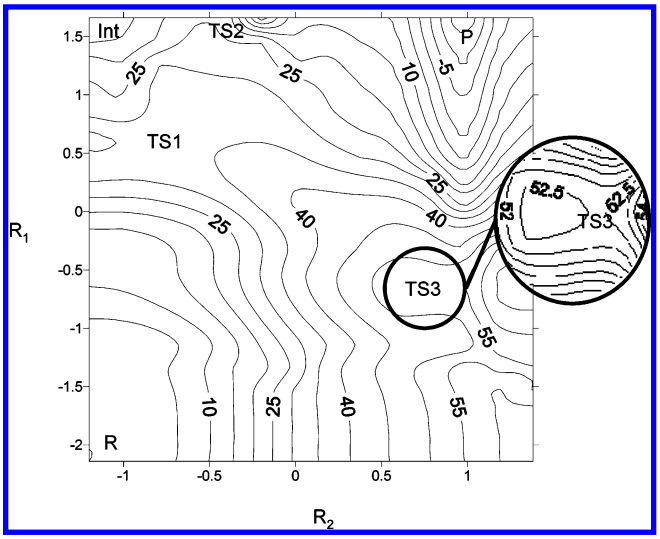

Figure 7. Potential energy surface at the AM1-IC/MM level. R_1 and R_2 are the coordinates (in Å) associated with the hydride and proton transfers (see text). The position of reactants (R), intermediate (Int), products (P), and transition state structures (TS1, TS2, and TS3) is qualitatively shown. Isoenergetical lines are depicted each 5 kcal/mol (0.5 kcal/mol in amplified zone).

Table 7. Relevant Distances (Å) and Relative Energies (kcal/mol) of the Stationary Structures Appearing on the PES Obtained at the AM1/MM Level with the Inclusion of Interpolated Corrections

	$r_{C_{nic}H_1}$	$r_{C_{pyr}H_1}$	$r_{N_{his}H_2}$	$r_{O_{pyr}H_2}$	energy
reactants	1.13	3.27	1.00	2.22	0
TS1	1.86	1.20	1.03	1.85	34
intermediate	2.80	1.15	1.00	2.22	13
TS2	2.79	1.13	1.11	1.53	24
products	2.79	1.13	1.98	0.99	−19
TS3	1.20	1.75	1.98	1.00	52

in gas phase obtained for the reduced QM model corresponding to the molecules presented in Figure 4. This new PES is presented in Figure 8, and the coordinates and relative energies of the stationary structures are gathered in Table 8. There are significant differences with the previous PESs. The most evident is that the intermediate appearing after the hydride transfer to the pyruvate has disappeared and a new intermediate (Int2) is found after the proton transfer. Thus, on the new PES the HP Pathway is a concerted mechanism taking place through a single transition state structure (TS4). This new transition state structure roughly corresponds to TS1 found on the previous PESs although it is now located at more advanced values of the proton-transfer coordinate. The PH Pathway is now described as a stepwise mechanism with two transition states (TS5 and TS6). The first corresponds to a very advanced proton transfer and the second to an early hydride transfer to the protonated intermediate (Int2). The energy of this structure is of about 37 kcal/mol above the reactants. At the reactant structure the carbon atom of pyruvate is found at a larger distance from the hydride (as in the PES with interpolated corrections). The products are now found at much larger values of the proton-transfer coordinate than in any of the discussed PES. This is due to the larger distance between histidine to the transferred proton. From the kinetic point of view, the concerted HP Pathway

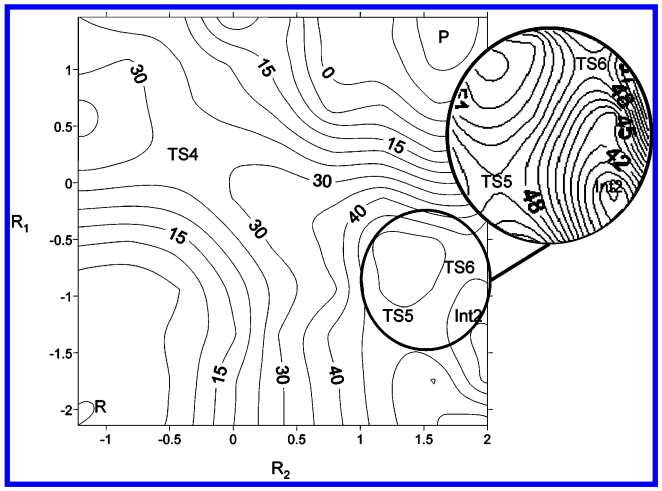

Figure 8. Potential energy surface obtained with bidimensional single-point MP2/6-31G(d,p) energy corrections. R_1 and R_2 are the coordinates (in Å) associated with the hydride and proton transfers (see text). The position of reactants (R), products (P), intermediate (Int2), and transition state structures (TS4, TS5, and TS4) is qualitatively shown. Isoenergetical lines are depicted each 5 kcal/mol (1 kcal/mol in amplified zone).

Table 8. Relevant Distances (Å) and Relative Energies (kcal/mol) of the Stationary Structures Appearing on the PES Obtained with Bidimensional MP2/6-31G(d,p) Single-Point Energy Corrections

	$r_{C_{nic}H_1}$	$r_{C_{pyr}H_1}$	$r_{N_{his}H_2}$	$r_{O_{pyr}H_2}$	energy
reactants	1.13	3.27	1.01	2.22	0
TS4	1.53	1.28	1.10	1.53	29
TS5	1.14	2.49	2.39	1.01	49
Int2	1.15	2.50	2.98	1.01	37
TS6	1.20	1.75	2.77	1.00	48
products	2.59	1.13	2.56	0.98	−13

seems to be the preferred mechanism on the PES (29 versus 48 kcal/mol).

It is interesting to comment on the performance of both correction methods when compared to the PES obtained with single-point corrections. Both the SVB and the IC schemes assume that differences between the high and low computational levels (MP2 and AM1 in this case) in the R_1 and R_2 coordinates are mutually independent. This is, the errors associated with the semiempirical description are expected to be approximately the same when the proton is transferred to the substrate (with charge −1 au) or to the intermediate (with a charge of −2 au). This is obviously not the case. However, despite the inherent deficiency both correction methods considerably improve the energetic description of both mechanisms when compared to the uncorrected AM1/MM PES. As compared to the PES obtained with bidimensional MP2 corrections, the AM1 surface has an average error in barrier heights of 15 kcal/mol and an average error in the four key geometrical variables at the two transition states of 0.32 Å. The SVB correction reduces these average errors to 4 kcal/mol and 0.31 Å, and the IC correction reduces them to 4 kcal/mol and 0.25 Å, respectively. It seems that separable correction schemes do a good job correcting the energies but not as well for correcting geometries of dynamical bottlenecks. This feature was already reported for the IC methodology,[18] and it seems that the SVB one presents a similar behavior. Anyway, the most important question is that both schemes are successfully predicting the HP Pathway as the preferred one, while on the uncorrected PES the PH Pathway displayed a lower energy barrier. The SVB method gives energy barriers in better agreement with the PES with bidimensional corrections for the HP Pathway, while the IC method agrees better with the bidimensional corrected PES in the PH Pathway.

Table 9. Interaction Energies (E_{int}, in kcal/mol) and Mulliken Charge on the Pyruvate (Q, in au) for the Complexes Formed between Pyruvate and Arg171 and Pyruvate and Arg109[a]

	Arg171/Pyr		Arg109/Pyr	
	E_{int}	Q	E_{int}	Q
HF/6-31G(d)	−111.21	−0.868	−68.76	−0.966
AM1	−98.37	−0.920	−62.80	−0.991
AM1/MM	−77.76	−1.000	−40.18	−1.000

[a] Geometries are taken from the reactant structure of the AM1/MM PES.

4.2. The Size of the QM Subsystem. The interaction between the substrate (pyruvate) and some residues in the MM part obviously play an essential role defining the possible reaction mechanisms. It has been proposed that the role of the Arg109 is to enhance the polarization of the pyruvate carbonyl group in the ground state and to stabilize the transition state in the HP Pathway, whereas the role of Arg171 is to assist in the binding of the substrate.[1,2] As previously described, when we tried to optimize the van der Waals parameters of the QM/MM interaction between pyruvate and water molecules we found a systematic deviation with respect to the QM values. This difference could be due to charge transfer effects, a term not included in standard QM/MM calculations. Obviously, this possible source of error requires some further studies in our system because the charge transfer could be even larger in the case of pyruvate surrounded by positively charged arginine residues. To address this issue we have compared the interaction energy between pyruvate and both arginines in the enzyme active site by means of gas-phase single-point energy calculations at the HF/6-31G(d) level, with those obtained at the AM1 and AM1/MM levels. These interaction energies are given in Table 9. As it can be seen, the AM1/MM calculations show important deviations from the HF values. The main contribution to this error is not the use of the AM1 Hamiltonian as the results are much improved when all the system is described by means of this semiempirical method. The magnitude of the error is directly correlated with the charge transfer (estimated from the Mulliken charges), and thus we attribute this error to the lack of charge-transfer effects in the QM/MM treatment.

Obviously, if the error is kept more or less constant all along the PES, then one could ignore this contribution. The charge of the substrate is the same in reactants (pyruvate) and products (lactate). However, it must be taken into account that after the hydride transfer the charge of the substrate increases from −1 to −2, and then the charge-transfer effect on the energy could be different in that region of the PES. For this reason we decided to explore again the AM1/MM

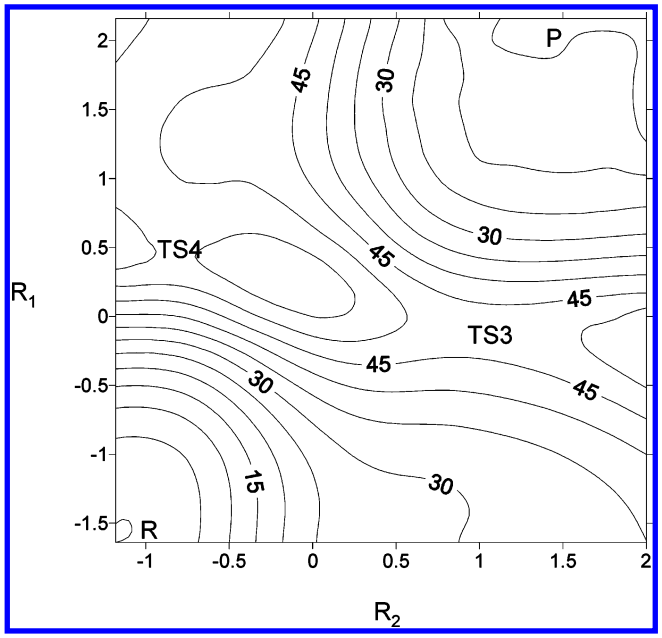

Figure 9. Potential energy surface obtained at the AM1/MM level with a QM region including Arg109 and Arg171. R_1 and R_2 are the coordinates (in Å) associated with the hydride and proton transfers (see text). The position of reactants (R), products (P), and transition state structures (TS3 and TS4) is qualitatively shown. Isoenergetical lines are depicted each 5 kcal/mol.

Table 10. Relevant Distances (Å) and Relative Energies (kcal/mol) of the Stationary Structures Appearing on the AM1/MM PES Obtained When the QM Region Includes Arg109 and Arg171

	$r_{C_{nic}H_1}$	$r_{C_{pyr}H_1}$	$r_{N_{his}H_2}$	$r_{O_{pyr}H_2}$	energy
reactants	1.13	2.77	1.01	2.17	0
TS4	1.78	1.22	1.03	1.81	54
TS3	1.36	1.39	2.01	0.99	47
products	3.08	1.12	2.40	0.98	13

2D uncorrected PES using the same reaction coordinates but increasing now the size of the QM region to include both Arg109 and Arg171 (resulting in a total of 78 QM atoms). This requires the introduction of two new GHOs placed at Cγ of each arginine. The new PES obtained for the larger QM subsystem is shown in Figure 9. As previously, we found two different mechanisms for the transformation of pyruvate into lactate: the HP Pathway and the PH Pathway in which the proton transfer precedes the hydride transfer. On this PES we only located two transition state structures (TS4 in the HP Pathway and TS3 in the PH Pathway), so both mechanisms are now described as concerted ones. The geometries and energies of the stationary structures are given in Table 10. The energy barrier in the HP Pathway (TS4) is about 54 kcal/mol and in the PH Pathway (TS3) is of about 47 kcal/mol. This description can be compared with the uncorrected AM1/MM PES with the smaller (52 atoms) QM subsystem. In that case the HP Pathway presented an energy barrier of about 52 kcal/mol associated with the first step (the hydride transfer), while the PH Pathway had a unique transition state structure with an associated energy barrier of about 41 kcal/mol (see Table 5). The reaction energy also changes noticeably, being of about −5 kcal/mol with the smaller QM subsystem and about 13 kcal/mol with the larger one. Then, the main effect of the inclusion of the arginines into the QM subsystem is to destabilize the intermediate which appeared after the hydride transfer, increasing the energy of that region of the PES. As a consequence the reaction path associated with the HP Pathway is now considerably more concerted than in our previous PES. All these changes can be rationalized considering that when Arg109 and Arg171 are described classically, electrostatic interactions with the intermediate obtained after the hydride transfer and with the protonated His195 are overestimated. This results in too large a stabilization of the intermediate, with a charge of −2, and also in too large an interaction with the protonated His195, with a positive charge. When these arginines are described quantum mechanically and the charge can be more delocalized, this overestimation of electrostatic interactions disappears, and thus the intermediate is no longer a minimum on the PES. This interpretation is confirmed by analysis of the charge distribution on the QM subsystem when it contains 52 or 78 atoms. For the intermediate, the absolute charge on the substrate is about 0.1 electrons smaller when the QM region includes both arginines. The magnitude of this charge transfer is confirmed by analysis of Mulliken and NPA charges[26,27] (a representation of the atomic charges for the stationary structures obtained at different levels is given as Supporting Information).

Because of the magnitude of the changes taking place when the size of the QM region was increased we decided to obtain a new PES for the large QM region including corrections to the AM1 description. According to the conclusions reached in the previous section we decided to include corrections by means of bidimensional single-point energy calculations at the MP2/6-31G(d,p) level, following the same procedure as before (see eq 12). The corrected PES is presented in Figure 10. The most relevant distances and the energies of the stationary structures corresponding to this PES are presented in Table 11. In this case we have an important difference with respect to the previously presented PESs: only one reaction mechanism is found. The unique transition state structure corresponds to a concerted hydride and proton transfers where the hydride transfer is considerably more advanced than the proton transfer, i.e., we have a concerted HP Pathway. The energy barrier is about 30 kcal/mol, and the reaction energy is close to zero (−0.7 kcal/mol).

5. Conclusions

We have here presented a QM/MM study of the PES corresponding to the pyruvate to lactate transformation catalyzed by LDH. This transformation takes place by means of a hydride and a proton transfer to the substrate. The order in which the hydride and the proton are transferred defines two different mechanistic routes for the process: a hydride transfer followed by a proton transfer (the so-called HP Pathway) and a proton transfer followed by a hydride transfer (the PH Pathway). Previous theoretical studies differ in the preferred mechanism as well as in their concerted or stepwise nature. For this reason we decided to improve the standard AM1/MM description of the reaction. In particular we have

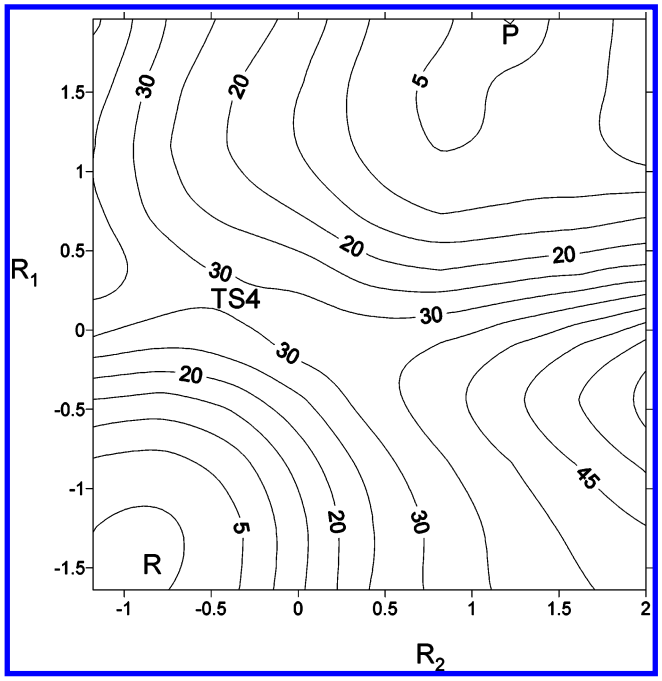

Figure 10. Potential energy surface obtained at the AM1/MM level with a QM region including Arg109 and Arg171 and bidimensional single-point MP2/6-31G(d,p) corrections. R_1 and R_2 are the coordinates (in Å) associated with the hydride and proton transfers (see eq 10). The position of reactants (R), products (P), and transition state structure (TS4) is qualitatively shown. Isoenergetical lines are depicted each 5 kcal/mol.

Table 11. Relevant Distances (Å) and Relative Energies (kcal/mol) of the Stationary Structures Appearing on the PES with Bidimensional MP2/6-31G(d,p) Single-Point Energy Corrections Obtained when the QM Region Includes Arg109 and Arg171

	$r_{C_{nic}H_1}$	$r_{C_{pyr}H_1}$	$r_{N_{his}H_2}$	$r_{O_{pyr}H_2}$	energy
reactants	1.13	2.77	1.01	2.17	0
TS4	1.62	1.26	1.12	1.50	30
products	3.06	1.12	2.20	0.95	−1

considered the effect of the van der Waals parameters used in the QM subsystem, the correction of the QM energy by two different schemes (SVB and IC), and the size of the QM subsystem to take into account charge-transfer effects.

While the change in the van der Waals parameters is quite modest, the inclusion of correction terms evaluated at the MP2 level into the AM1 energy has important consequences on the studied PES. The PH Pathway presents a lower energy barrier on the uncorrected AM1/MM PES, but when both correction schemes are considered the HP Pathway presents noticeably lower energy barriers. However, both correction schemes display some deficiencies associated with the fact that the correction energies associated with the proton and the hydride transfer coordinates are taken as independent. The most important consequence is that both methods describe the HP Pathway as a stepwise mechanism, while it appears as a concerted one when corrections with single-point calculations on the whole PES at the MP2 level are carried out. This feature of the PES is stressed when the QM subsystem is enlarged to include also Arg109 and Arg171. A classical description of these two residues results in an overstabilization of the structure appearing after the hydride transfer to the substrate. Note that the terms stepwise and concerted refer here just to the presence or absence, respectively, of an intermediate on the PES. Indeed, only a dynamical study could show the actual relevance of the intermediate for the reaction mechanism.

Thus, in our best treatment, the pyruvate to lactate transformation catalyzed by LDH is described as a concerted hydride and proton transfer mechanism with a single transition structure where the hydride transfer is considerably more advanced than the proton transfer. However, the mechanistic details depend on the particular computational level chosen to describe the process. The energy barrier found is of about 30 kcal/mol, a value that seems to be overestimated when compared to the experimental estimations of the activation free energy barrier (with an upper limit of about 15 kcal/mol[28]). Entropic contributions, tunneling, higher QM level, and a better QM/MM description are expected to contribute to diminish the gap with the experimental estimations. The protonation state of some residues close to the active site, here assumed to be found in their standard protonation states at pH 7, could also be a source of discrepancy with experiments. Studies are underway to evaluate all these contributions. In any case, and as a methodological conclusion of the present work, dynamical treatments of this system should be carried out on a PES including high level corrections to the QM energy for the proton and the hydride transfers, and, importantly, these corrections should not be included independently in order to have an accurate description.

Acknowledgment. Authors thank Prof. D. G. Truhlar for reading and commenting the manuscript. We thank the DGI for projects DGI BQU2003-04168-C03 and BQU-2002-00301, BANCAIXA for project P1A99-03, and Generalitat Valenciana for project GV01-324, GV04B-21, GV04B-131, and GRUPOS04/28. S.F. and J.J.R.-P. acknowledge a doctoral fellowship of the Ministerio de Ciencia y Tecnología. S.F. also acknowledges the Ministerio for financial support during her visit to the UAB and the warm hospitality of all the people of the Departament de Química of the Universitat Autònoma de Barcelona.

Supporting Information Available: Geometries (in Å) and absolute energies at the HF/6-31G(d,p) level (in au) of the complexes shown in Figure 3, energy profiles (kcal/mol) obtained using the $R_1 + R_2 = R_4$ coordinate, and atomic charges (in au) obtained for stationary structures of the HP pathway. This material is available free of charge via the Internet at http://pubs.acs.org.

References

(1) Clarke, A. R.; Atkinson, T.; Holbrook, J. J. *Trends Biochem. Sci.* **1989**, *14*, 145−148.

(2) Burger, J. W. I.; Ray, W. J. J. *Biochemistry* **1984**, *23*, 3620−3626.

(3) Moliner, V.; Turner, A. J.; Williams, I. H. *Chem. Commun.* **1997**, 1271−1272.

(4) Moliner, V.; Williams, I. H. *Chem. Commun.* **2000**, 1843−1844.

(5) Turner, A. J.; Moliner, V.; Williams, I. H. *Phys. Chem. Chem. Phys.* **1999**, *1*, 1323−1331.

(6) Ranganathan, S.; Gready, J. E. *J. Phys. Chem. B* **1997**, *101*, 5614−5618.

(7) Ranganathan, S.; Gready, J. E. *J. Chem. Soc, Faraday Trans.* **1994**, *90*, 2047−1456.

(8) Yadav, A.; Jackson, R. M.; Holbrook, J. J.; Warshel, A. *J. Am. Chem. Soc.* **1991**, *113*, 4800−4805.

(9) Truhlar, D. G.; Gao, J. L.; Garcia-Viloca, M.; Alhambra, C.; Corchado, J.; Sanchez, M. L.; Poulsen, T. D. *Int. J. Quantum Chem.* **2004**, *100*, 1136−1152.

(10) Field, M. J.; Bash, P. A.; Karplus, M. *J. Comput. Chem.* **1990**, *11*, 700−733.

(11) Gao, J.; Thompson, M. A. *Combined quantum mechanical and molecualr mechanical methods*; Washington, DC, 1988.

(12) Gao, J.; Amara, P.; Alhambra, C.; Field, M. J. *J. Phys. Chem. A* **1998**, *102*(24), 4714−4721.

(13) Dewar, M. J. S.; Zoebisch, E. G.; Healy, E. F.; Stewart, J. J. P. *J. Am. Chem. Soc.* **1985**, *107*, 3902−3909.

(14) Gonzalez-Lafont, A.; Truong, T. N.; Truhlar, D. G. *J. Phys. Chem.* **1991**, *95*, 4618−4627.

(15) Devi-kesavan, L. S.; Garcia-Viloca, M.; Gao, J. *J. Theor. Chem. Acc.* **2003**, *109*, 133−139.

(16) Poulsen, T. D.; Garcia-Viloca, M.; Gao, J.; Truhlar, D. G. *J. Phys. Chem. B* **2003**, *107*, 9567−9578.

(17) Ruiz-Pernia, J. J.; Silla, E.; Tuñón, I.; Martí, S.; Moliner, V. *J. Phys. Chem. B* **2004**, *108*, 8427−8433.

(18) Chuang, Y.; Corchado, J. C.; Truhlar, D. *J. Phys. Chem. A* **1999**, *103*, 1140−1149.

(19) Corchado, J. C.; Coitiño, E. L.; Chuang, Y.; Fast, P. L.; Truhlar, D. *J. Phys. Chem. A* **1998**, *102*, 2424−2438.

(20) Wigley, D. B.; Gamblin, S. J.; Turkenburg, J. P.; Dodson, E. J.; Piontek, K.; Muirhead, H.; Holbrook, J. J. *J. Mol. Biol.* **1992**, *223*, 317−335.

(21) Brooks, B. R.; Bruccoleri, R. E.; Olafson, B. D.; States, D. J.; Swaminathan, S.; Karplus, M. J. *J. Comput. Chem.* **1983**, *4*, 187−217.

(22) Jorgensen, W. L.; Chandrasekhar, J.; Madura, J.; Impey, R. W.; Klein, M. L. *J. Chem. Phys.* **1983**, *79*, 926−935.

(23) Freindorf, M.; Gao, J. *J. Comput. Chem.* **1996**, *17*, 386-395.

(24) Gao, J.; Xia, X. *Science* **1992**, *258*, 631−635.

(25) Frisch, M. J.; Trucks, G. W.; Schlegel, H. B.; Gill, P. M. W.; Johnson, B. G.; Robb, M. A.; Cheeseman, J. R.; Keith, T.; Peterson, G. A.; Montgomery, J. A.; Raghavachari, K.; Al-Laham, M. A.; Zakrzewski, V. G.; Ortiz, J. V.; Foresman, J. B.; Cioslowski, J.; Stefanov, B. B.; Nanayakkara, A.; Challacombe, M.; Peng, C. Y.; Ayala, P. Y.; Chen, W.; Wong, M. W.; Andres, J. L.; Replogle, E. S.; Gomperts, R.; Martin, R. L.; Fox, D. J.; Binkley, J. S.; Defrees, D. J.; Baker, J.; Stewart, J. P.; Head-Gordon, M.; Gonzalez, C.; Pople, J. A. Pittsburgh, PA, 1995.

(26) Reed, A. E.; Curtis, L. A.; Weinhold, F. *Chem. Rev.* **1988**, *88*, 899−926.

(27) Foster, J. P.; Weinhold, F. *J. Am. Chem. Soc.* **1980**, *102*, 7211−7218.

(28) Clarke, A. R.; Wigley, D. B.; Chia, W. N.; Barstow, D.; Atkinson, T.; Holbrook, J. J. *Nature* **1986**, *324*, 699−702.

CT050016L